Numerical Study of Different Types of Focused Wave Breaking on a Cylinder

Lige Zhao; Alistair G. L. Borthwick; Deborah M. Greaves
School of engineering computing and mathematics, University of Plymouth, Plymouth, UK
lige.zhao@plymouth.ac.uk

HIGHLIGHTS

We numerically investigate three different types of phase-focused wave breaking on a cylinder with regard to wave frequency, Courant number, structural diameter, distance between the breaking position and the structure, and KC number. A similar variation of breaking force with the distance and KC number is observed in three cases.

1 INTRODUCTION

Wave breaking is a form of instability, whose onset is often described by means of empirical breaking criteria developed from statistical observations. At present, our knowledge of the interaction between breaking wave and the water body remains incomplete. Ghadirian et al.(2016) [1] studied focused wave breaking using a combination of two open source tools, OpenFOAM and OceanWave3D. Ghadirian et al. used Goda's breaking criteria to create a steep wave based on the JONSWAP spectrum with an extremely high value of significant wave height (Hs), and examined the instant at which maximum pressure was experienced on a cylinder and visualised the water free surface around the column and estimated the stagnation pressure. Likewise, Cui et al.(2022) [2] used REEF3D and Large Eddy Simulation models to study focused wave breaking, and examined geometric, kinematic and dynamic criteria for breakers of different steepness. Recently, Batlle Martin et al.(2023) [3] simulated focused wave breaking using fully non-linear potential flow (FNPF) theory. They validated their model by comparing the predicted surface elevation at one wave gauge and the inline force on several column segments against experimental data. Batlle Martin et al. analysed the relationships between breaking severity, curling factor and slamming pressure. The foregoing numerical studies utilized different scale ratios, different types of wave spectrum, different focused wave theories or different frequency band widths. This paper uses simulations obtained using the open source tool OpenFOAM with the GABC wave boundaries to verify the aforementioned breaking wave cases. The incipient breaking wave distance from the structure, and Keulegan-Carpenter (KC) number are studied, leading to a more complete understanding of the interaction of focused waves with ocean structures.

2 MODEL SET-UP AND VALIDATION

In the Numerical Wave Tank (NWT), the wave generation and absorption use a *generation and absorbing boundary condition* (GABC) method, which was proposed by Borsboom et al in 2021 [4]. GABC has a low reflection coefficient (less than 5%) over a very broad range of the non-dimensional wave number. The absence of a relaxation zone in the wave tank leads to lower computational overhead. Neumann and no-slip wall boundary conditions are implemented at the side and bottom walls for the pressure and velocity respectively.

symmetry condition is applied at the front side wall, enabling us to simulate half the domain. In OpenFOAM, the Navier-Stokes equations are solved using the Finite Volume Method (FVM) with a PIMPLE iteration approach. The VOF method is used to capture the free surface. A second-order scheme is applied to the free surface volume fraction to accurately represent the interface while minimizing numerical diffusion. All other terms utilize first-order schemes for computational stability. For turbulence closure, a $k-\omega$ SST RANS model is implemented. In all 2D empty tank cases, we use MPI across 128 CPUs with a processor clock speed of 2.5 GHz; the 3D cases use 256 CPUs.

We now introduce the three breaking cases used to validate the model. Table 1 summarises the wave parameters and the convergent numerical mesh settings. Figure 1 illustrates the set-ups for the three cases including the positions of wave gauges (WG). By definition, the linear focused wave is composed of the superposition of linear wave components: $\eta(x,t) = \sum_{n=1}^{N} a_n \cos\left[k_n(x-x_0) - \omega_n(t-t_0)\right]$.

Case	A	B	C
$d(m)$	33	0.54	2
W/d	2.12	0.74	2.00
L/d	15.15	18.52	15.00
Frequency range $f/(\sqrt{(g/d)})$	[0.073, 0.55]	[0.235, 0.563]	[0.005, 0.361]
f_{num}	87	128	80
A_{cr}/d	0.27	0.06	0.14
Global steepness	0.42	0.57	0.32
Group speed $C_g/(\sqrt{(gd)})$	0.24	0.17	0.33
Refinment height z/A_{cr}	2.5	2.5	2.5
Min mesh size (m^3)	$A_{cr}/22^3$	$A_{cr}/14^3$	$A_{cr}/23^3$
Total cell num	1.3 M	1.4 M	1.8 M

Table 1: Non-dimensional parameters of the three cases

Figure 2A shows the predicted time series of free surface elevation, in-line force and the experimental data obtained by Ghadirian et al, who create the focused wave series using NewWave theory, where $a_n = \frac{A_0 S_\eta(\omega_n)\delta\omega}{\sum_{n=1}^{N} S_\eta(\omega_n)\delta\omega}$, and $A_0 = \sqrt{2m_0 \log(N)}$. Close agreement is evident between the two sets of results, with the focused point of the simulation shifted 35 m downward compared with the experiment. Figure 2B shows the corresponding numerical predictions and experimental measurements for a case examined by Cui et al. who created the focused wave from the Constant Wave Steepness (CWS) spectrum, with global steepness $\epsilon = 0.57$ and wave amplitude determined according to $\epsilon/f_{num} = k_n a_n$, which decreases as the wave frequency increases. The surface elevation at 2 WGs are in good agreement with the experiment. The final sets of results in Figure 2 relate to the case considered by Batlle Martin et al. who created their focused wave using the theory by Rapp et al.(1990) [5]. The amplitude extracted from JONSWAP spectrum where the equation $H_s = \frac{1}{16}\sum S_\eta(f_n)\mathrm{d}f$ is satisfied. It can be seen that the predicted free surface elevation at the WG and the slamming force on four segments are all in good agreement with the experimental data.

3 RESULTS

Simulating cases are summarised in table 2, including various Co number, cylinder diameters D and the incipient breaking wave distance from the structure δ. We normalize the wave parameters and the structure scale using the KC number $\frac{C_g T_c}{D}$ to compare the inline force of

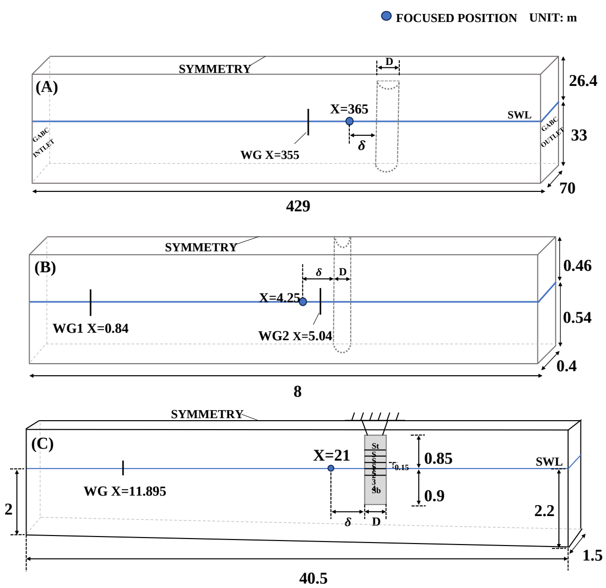

Figure 1: Diagram of the numerical settings of the three cases

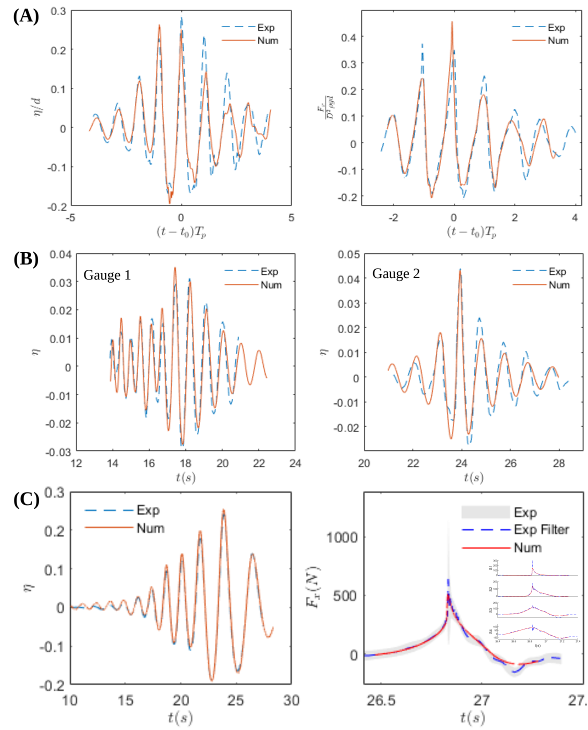

Figure 2: Validation of the three cases

the three breaking cases, which use different wave theories and scaling ratios.

The results are shown in Fig 3. The maximum inline force F_x is non-dimensionalised as $\hat{F} = \frac{F_x}{\rho g A_{cr} D^2}$. Here, F_x is the wave force above the still water line, representing the wave slamming area. Fig 3(a) shows a 3% difference in $\hat{F}$ between Co 0.05 and 0.5. It was observed that Co affects the breaking onset position, resulting in about 1 m displacement in case C. However, this instability has minimal impact on $\hat{F}$. Fig 3(b) shows the similar tendency in cases A, B and C, that maximum $\hat{F}$ exists at certain non-dimensional δ. Fig 3(c) plots the $\hat{F}$ for three cases under different KC number, a positive correlation is observed. Case A exhibits a higher $\hat{F}$, as it is simulated at the sea scale, potentially leading to a stronger inertia effect and a larger curling factor. In Fig 3(d), we further scale down $\hat{F}$ with the KC number. For Cases A and C, both of which employ the JONSWAP spectrum with a wider bandwidth, the dimensionless inline forces become more stable, indicating that the inline force is not influenced by the KC number. However, case B, which uses the CWS spectrum, does not show this trend.

4 CONCLUSION

In this work, we investigated three published cases of focused wave breaking, drawing the following conclusions:

1. Our model shows good agreement with the three different focused wave breaking cases.

2. We found that the maximum inline force occurs when the cylinders are positioned at similar dimensionless locations.

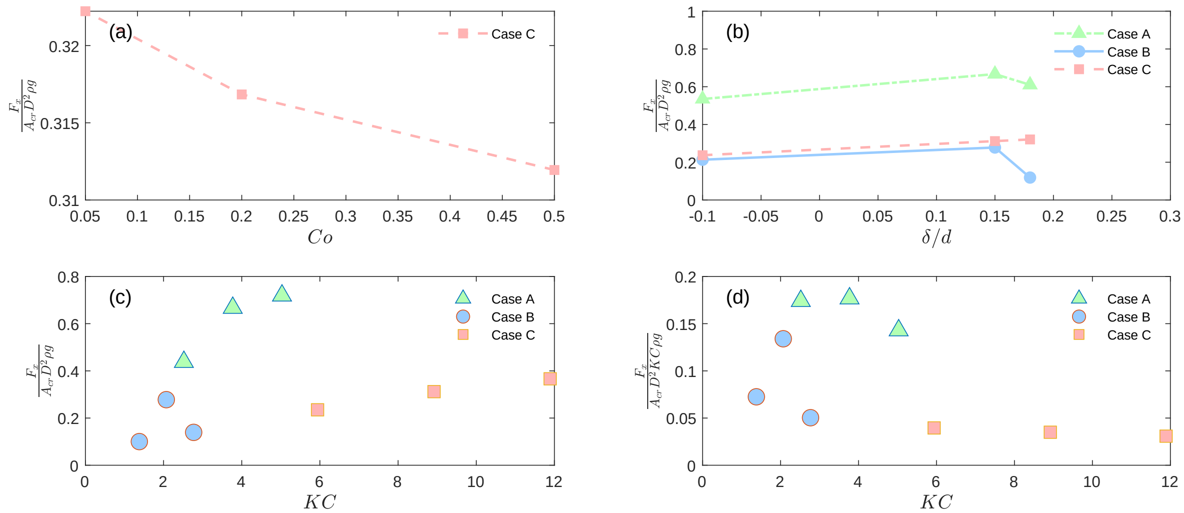

Figure 3: Relationship between the non-dimensional inline force and Co number, δ/d, and KC number for the three cases

	A					B			
	1	2	3	4	5	1	2	3	4
D/d	0.2	0.3	0.15	0.2	0.2	0.2	0.3	0.15	0.2
δ/d	0.15	0.15	0.15	-0.1	0.18	0.15	0.15	0.15	-0.1
KC	2.07	1.38	2.77	2.07	2.07	8.92	5.94	11.89	8.92
	B			C					
	5	6	7	1	2	3	4	5	
Co	0.5	0.2	0.05	0.5	0.5	0.5	0.5	0.5	
D/d	0.2	0.2	0.2	0.2	0.3	0.15	0.2	0.2	
δ/d	0.18	0.15	0.15	0.15	0.15	0.15	-0.1	0.18	
KC	8.92	8.92	8.92	3.77	2.52	5.03	3.77	3.77	

Table 2: Configurations of non-dimensional diameter, δ, KC, and Co number for three cases

3. For the JONSWAP spectrum cases, the dimensionless inline force shows a positive correlation with the KC number.

Further studies will be carried out to quantify the relationships between $\hat{F}$, the KC number, scaling ratios, and the curling factor. For CWS spectrum-induced focused wave breaking, a detailed study on its wave interaction effects will be essential.

REFERENCES

[1] Ghadirian, A., Bredmose, H., and Dixen, M. *Breaking Phase Focused Wave Group Loads on Offshore Wind Turbine Monopiles*. 092004.

[2] Cui, T., He, G., Jiang, M., Wang, W., Yuan, L., Han, D., Kamath, A., and Bihs, H. *Large Eddy Simulation of Focused Breaking Waves with Different Wave Steepness*. 102122.

[3] Batlle Martin, M., Harris, J. C., Filipot, J.-F., Hulin, F., Tassin, A., and Renaud, P. *Deep Water Focused Breaking Wave Loads on a Fixed Cylinder*. 104397.

[4] Borsboom, M., and Jacobsen, N. G. *A Generating-Absorbing Boundary Condition for Dispersive Waves*. 2443–2467.

[5] Rapp, R., and Melville, W. *Laboratory Measurements of Deep-Water Breaking Waves*.